

# Optimizing MABR operation for efficient tetracycline and nutrient removal in wastewater

Ya-Jun Chen<sup>1†</sup>, Yi-Kun Wang<sup>1,2†</sup>, Yao Pan<sup>1</sup>, Jin Zhou<sup>4</sup>, Peng-Sheng Miao<sup>\*\*3</sup> and Hai-Yin YU<sup>\*1</sup>

<sup>1</sup>College of Chemistry and Materials Science, Anhui Normal University, 189 Jiu Hua Nanlu, Wuhu, Anhui 241002, China

<sup>2</sup>Zhejiang University of Science and Technology, 318 Liuhe road, Hangzhou, Zhejiang, 310023, China

<sup>3</sup>Anhui HuaShang Cable Technology Co., Ltd, Bawan industrial Zone, Gaogou Town, Wuwei City, Wuhu City, Anhui Province, 238339, P.R. China

<sup>4</sup>Department of Material and Chemical Engineering, Chizhou University, Chizhou 247000, China

(Received November 21, 2024, Revised July 9, 2025, Accepted September 30, 2025)

**Abstract.** The escalating pollution from pharmaceutical wastewater, notably tetracycline (TC), demands innovative treatment solutions. This study explores a membrane aerated biofilm reactor (MABR) for TC biodegradation and simultaneous removal of total nitrogen (TN), ammonia nitrogen ( $\text{NH}_4^+\text{-N}$ ), and total phosphorus (TP). The MABR employed polypropylene hollow fiber membranes (0.2  $\mu\text{m}$  pore size) to develop stratified biofilms enabling microbial synergy: aerobic nitrifiers degraded  $\text{NH}_4^+\text{-N}$  while anoxic denitrifiers reduced TN. Optimal conditions (0.122 MPa aeration, 16-h HRT, 0.4 mg/L TC) achieved 70% TC degradation, 90%  $\text{NH}_4^+\text{-N}$  removal, 88% TN removal, 75% TP removal, and 93% COD removal. Microbial analysis confirmed TC mineralization via synergistic biofilm communities, minimizing toxic byproducts. The system's energy-efficient oxygen diffusion (direct membrane aeration) and high contaminant-removal efficiency underscore its cost-effectiveness. These findings position MABR as a sustainable, non-toxic solution for complex wastewater treatment.

**Keywords:** biodegradation; denitrification; membrane aerated biofilm reactor (MABR); nitrification; tetracycline (TC)

## 1. Introduction

Antibiotics, integral components of drugs and personal care products, infiltrate the environment from various sources. Human consumption leads to a portion of antibiotics being excreted unchanged or as metabolites into urban sewage (Ahmed *et al.* 2020). Medical facilities discharge wastewater and waste residues teeming with antibiotics, and the extensive use in animal husbandry exacerbates environmental pollution (Mei *et al.* 2020). Wastewater containing tetracycline (TC) is especially concerning as it can induce drug-resistant bacteria, disrupt ecological balance, and impact organisms (Machat *et al.* 2019).

Existing treatment technologies for such wastewater have notable limitations. Conventional physical and chemical methods often demand high energy consumption and generate secondary pollutants. Advanced oxidation processes, for example, can be costly and may not fully mineralize antibiotics (Celik *et al.* 2018). Biological treatment methods, while generally more eco-friendly, struggle to degrade recalcitrant antibiotics like TC.

Membrane aerated biofilm reactors (MABRs) present unique benefits. The membrane in an MABR functions as both an immobilization carrier and a microporous aerator. Oxygen and contaminants diffuse in opposite directions, creating separate ecological niches for anaerobic and aerobic microorganisms within the biofilm (Ghasemi *et al.* 2023). This spatial stratification minimizes excessive biofilm growth during the treatment of high-strength organic wastewater and enables the effective degradation of refractory compounds through the cooperation of different functional microorganisms (Alonso and Lackner, 2019).

This study aims to explore the application of an MABR in the biodegradation of TC and the simultaneous removal of total nitrogen (TN), ammonia nitrogen ( $\text{NH}_4^+\text{-N}$ ), and total phosphorus (TP) from wastewater. We examine the effects of  $\text{O}_2$  gas pressure and hydraulic retention time on treatment efficiency, evaluate transformation products, and analyze the microbial culture. Our goal is to develop an efficient, cost-effective, and environmentally friendly treatment approach for antibiotic-laden wastewater.

## 2. Materials and Methods

### 2.1 Membrane aerated biofilm reactor and operation

The experimental setup of the membrane aerated biofilm reactor (MABR) is detailed in Fig. 1. The MABR consists of an organic glass cylinder with a diameter of 6 cm and a height of 50 cm, having a volume of 1.41 L. The membrane

\*Corresponding author, Professor  
E-mail: yhy456@ahnu.edu.cn

\*\*Co-corresponding author, Ph.D.,  
E-mail: hs\_mps0106@163.com

†Co-first author

Table 1 The specific experimental conditions

Experimental Period	Duration (days)	Hydraulic Retention Time (HRT, h)	Oxygen Pressure (MPa)	Tetracycline Concentration (mg/L)	Ammonium Loading (mg/m <sup>2</sup> ·d)
P1	1~15	24	0.041	0.4	260.2
P1	16~25	18	0.027	0.4	260.2
P1	26~35	18	0.014	0.4	260.2
P2	36~45	15	0.041	0.4	260
P2	46~55	15	0.027	0.4	260
P2	56~65	15	0.014	0.4	260
P3	66~75	10	0.041	0.4	386.4
P3	76~85	10	0.027	0.4	386.4
P3	86~95	10	0.014	0.4	386.4
P4	96~105	7.5	0.041	0.4	510.6
P4	106~115	7.5	0.027	0.4	510.6
P4	116~125	7.5	0.014	0.4	510.6
P5	126~135	18	0.041	0.5	510.6
P5	136~145	18	0.041	0.3	510.6
P5	146~155	18	0.041	0.1	510.6

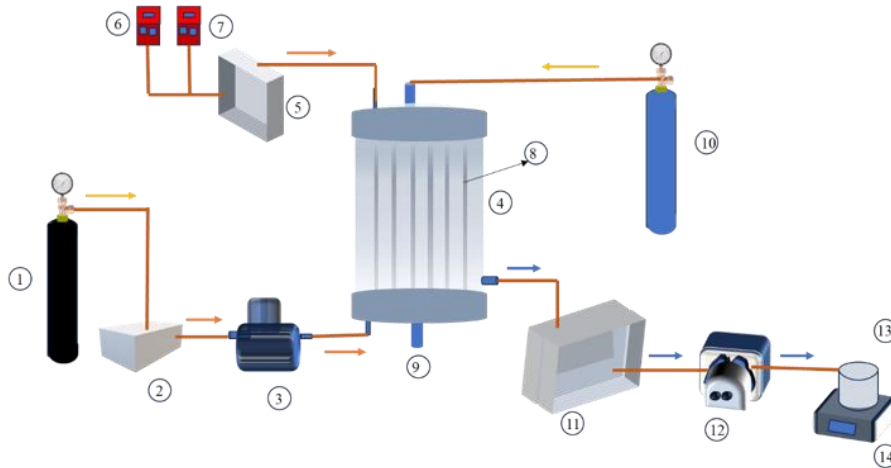


Fig. 1 The diagram of the membrane aeration biofilm reactor

module is composed of 120 polypropylene hollow fiber membranes, each 50 cm long, with a thickness of about 30 - 40  $\mu\text{m}$  and a pore size of 0.2  $\mu\text{m}$ . The system consists of the following parts: 1, N<sub>2</sub> bottle for nitrogen supply; 2, feed tank for storing synthetic wastewater; 3, influent pump for feeding wastewater; 4, the MABR; 5, pH and DO connector; 6 and 7, pH and dissolved oxygen probe; 8, hollow polypropylene membrane module for biofilm attachment and gas transfer; 9, exhaust gas outlet for released gases; 10, O<sub>2</sub> bottle for oxygen supply; 11, filtrate for the withdrawing solution; 12, pump for withdrawing treated solution; 13, container for collected treated water; 14, the electronic balance, which is employed to measure the weight change of the draw solution, enabling the determination of the effluent flow rate, which is essential for monitoring and controlling the hydraulic conditions in the MABR system.

The synthetic wastewater circulates between a sealed

feed tank filled with nitrogen and the biofilm reactor, facilitated by a peristaltic pump. Oxygen is supplied by an oxygen cylinder to regulate the pressure inside the fiber. During operation, the influent pH is maintained at around 8, and the experiment is conducted at about  $25 \pm 2$  °C by placing the entire experimental setup within a thermostatic laboratory.

The inoculated sludge is added to the reactor, with only 20 mg/L added during the one-week nitrification period. The biofilm forms at an HRT of 24 h and an oxygen pressure of 0.041 MPa. After the nitrification adaptation period, antibiotics are introduced. Different HRTs and oxygen pressures are adjusted to study the degradation of antibiotics and nitrogen removal. The degradation of wastewater, as well as nitrification and denitrification reactions, primarily occur on the biofilm, the structure of which is shown in Fig. 2. The specific experimental conditions are presented in Table 1.

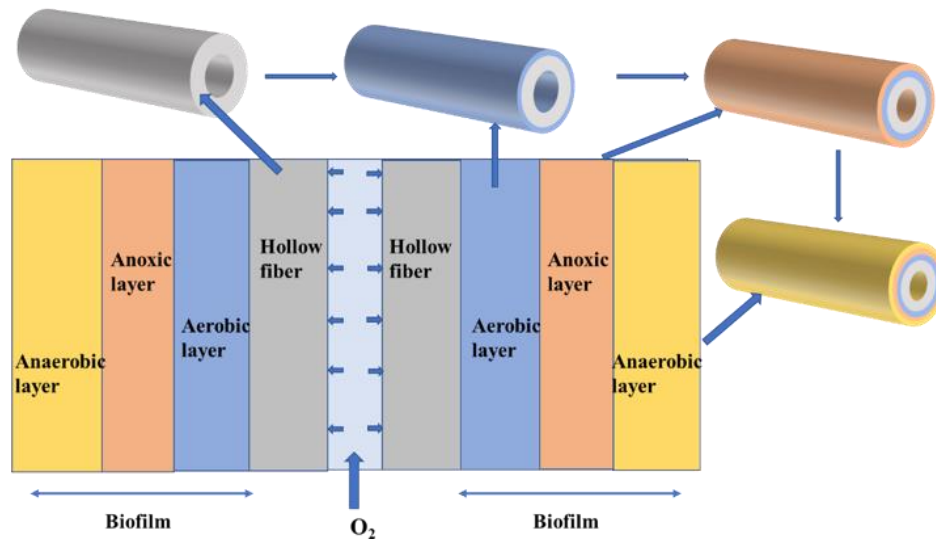


Fig. 2 Biofilm structure formation on the membrane surface

## 2.2 Preparation of synthetic wastewater

The synthetic wastewater is prepared by dissolving the following reagents: 6.4 g  $\text{NH}_4\text{Cl}$ , 0.3865 g  $\text{Cr}(\text{NO}_3)_3 \cdot 9\text{H}_2\text{O}$ , 0.0542 g  $\text{MnSO}_4 \cdot \text{H}_2\text{O}$ , 0.1043 g  $\text{ZnCl}_2$ , 0.0503 g  $\text{PbCl}_2$ , 0.1683 g  $\text{Ni}(\text{NO}_3)_2 \cdot 6\text{H}_2\text{O}$ , 45.85 g  $\text{CH}_4\text{N}_2\text{O}$ , 61 g Starch, 57.5 g Powdered Milk, 8.7 g Peptone, 26.05 g Yeast extract, 39.55 g  $\text{CH}_3\text{COONa}$ , 14.5 g  $\text{MgHPO}_4 \cdot 3\text{H}_2\text{O}$ , 11.6 g  $\text{KH}_2\text{PO}_4$ , 2.89 g  $\text{FeSO}_4 \cdot 7\text{H}_2\text{O}$ , 0.2655 g  $\text{CuCl}_2 \cdot 2\text{H}_2\text{O}$ . These are dissolved in a 500 mL beaker, stirred until dissolved, and then the volume is fixed in a 1000 mL flask. The solution is shaken well, poured into a bottle, and stored in the refrigerator (Yu *et al.* 2005).

## 2.3 Analysis methods

Dissolved oxygen (DO), chemical oxygen demand (COD), ammonia nitrogen ( $\text{NH}_4^+\text{-N}$ ), and sludge concentration (Abu Hasan *et al.* 2020). The contents of ammonium, nitrite, and nitrate are determined by spectrophotometer. COD is measured using the potassium dichromate method. DO is detected with an oxygen analyzer (JPB - 607A, Shanghai Yidian Scientific Instrument Co., Ltd).

For the determination of the steady state of the reactors, we continuously measured the removal rates of key pollutants including COD, TN, TP, and TC at regular intervals. When the removal rates exhibited a stable trend with less than 5% variation in three consecutive measurements, the reactor is considered to reach a steady state. Regarding the different operation durations under various HRTs, this design was intended to comprehensively investigate the impact of HRT on the degradation process. By observing the reactors' performance at different stages of the reaction under different HRTs, we aimed to capture the dynamic changes of the system and gain a more in-depth understanding of the reaction kinetics. This approach allowed us to explore a wider range of conditions and obtain more valuable data for analyzing the relationship between HRT and the degradation efficiency.

## 3. Results and discussions

### 3.1 Oxygen permeation of hollow fiber membranes and bubble point testing

#### 3.1.1 Oxygen transfer kinetics

Initially, purge the clean water with a continuous flow of nitrogen gas to remove dissolved oxygen. Subsequently, utilize a peristaltic pump to meticulously inject the degassed clean water into the MABR. At a pressure of 0.120 MPa, continuously introduce pure oxygen into the water while simultaneously employing a DO meter to monitor the DO levels in real-time. Log the DO values at five-minute intervals to meticulously chart the oxygen saturation trends. Fig. 3 shows the variation of dissolved oxygen (DO) concentration over time in the membrane aerated biofilm reactor (MABR). The purpose is to illustrate the dynamic process of oxygen transfer and its stabilization during the operation of the reactor, which is closely related to the biofilm formation and the degradation of pollutants. It helps to understand the performance and oxygen utilization characteristics of the MABR. The DO in the biofilm reactor initially increases exponentially, then grows more slowly, and finally stabilizes at around 11 mg/L.

#### 3.1.2 Bubble point analysis

Subsequently, we started introducing oxygen pressure from zero and gradually increased the oxygen pressure, observing for the formation of bubbles. The pressure at which bubbles eventually formed was 0.152 MPa.

The theoretical bubble point pressure for a 0.2  $\mu\text{m}$  membrane can be estimated using the Young - Laplace equation. However, in our experiment, bubbles were observed at 0.152 MPa. This discrepancy could be attributed to several factors. The actual membrane might have some irregularities or defects that lower the effective bubble point pressure compared to the theoretical value calculated based on an ideal membrane. Additionally, the presence of impurities or contaminants in the system could also affect the bubble formation behavior. Further

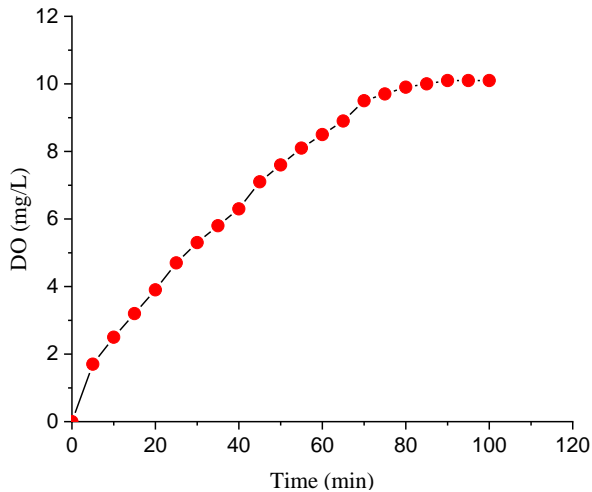


Fig. 3 Evolution of DO concentration over time at an oxygen gas pressure of 0.120 MPa

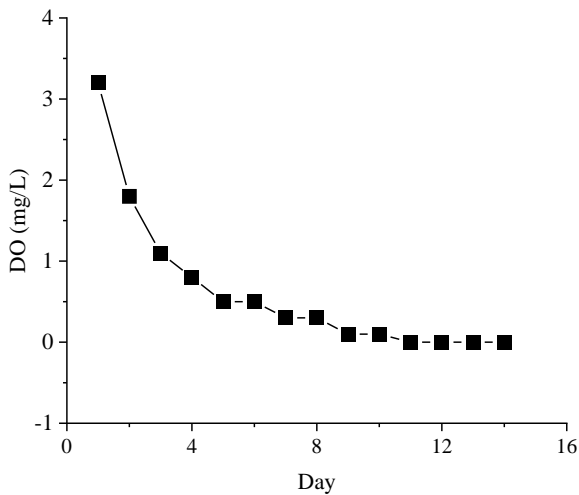


Fig. 4 DO change during reactor startup

investigation is needed to fully understand this deviation and its implications for the membrane's performance in our experimental setup.

### 3.1.3 Biofilm development dynamics

The DO change during the startup of the reactor is presented in Fig. 3. By observing this trend, we can monitor the progress of biofilm formation and the consumption of oxygen by microorganisms. This data is essential for evaluating the initial stage of the MABR operation and understanding the relationship between oxygen and the biological processes occurring in the reactor. As shown in Fig. 4, during the first two d after the activated sludge is introduced, the DO value is not zero but keeps decreasing. This is because when the MABR is initially started, the biofilm has not yet begun to form, there are fewer aerobic bacteria, and the oxygen directly diffuses into the liquid without being completely consumed. As the aerobic bacteria increase and the aerobic layer forms, the DO content in the MABR keeps decreasing until the biofilm is fully formed and the DO is completely consumed, resulting in a DO value of zero (Tian *et al.* 2015).

To better understand the oxygen transfer and utilization in the MABR, we measured and presented the DO vs time data in Fig. 3 and Fig. 4. The changes in DO concentration reflect the dynamic processes during the startup and stable operation of the reactor.

In the early stage (Fig. 4), the decreasing DO indicates the active consumption of oxygen by microorganisms involved in biofilm formation. As the biofilm matures, the DO stabilizes (Fig. 3), which provides insights into the oxygen balance and the overall performance of the MABR. This information is crucial for optimizing the operating conditions and evaluating the effectiveness of the treatment process.

### 3.2 Sludge acclimation and biofilm formation

Take 100 mL of sludge from the bacterial tank and then filter it using a vacuum pump. Place the resulting solid in an oven to dry, and finally remove it and weigh it to calculate Mixed Liquor Suspended Solids (MLSS), which is determined to be 7800 mg/L. Transfer the acclimated sludge to the MABR for intermittent treatment to cultivate the formation of a biofilm, adding culture fluid once every 24 h for two consecutive weeks. The pressure of oxygen introduced into the MABR is controlled at 0.122 MPa, and the amount of OTC added is maintained at 1.70 mg/L. Sample daily for DO and pH testing until the DO stabilizes at zero before commencing regular wastewater testing.

### 3.3 Removal rate of COD

The COD removal efficiency under varying oxygen pressures and HRTs is show in Fig. 5, as can be seen that it exhibited complex patterns.

When the oxygen pressure was 0.114 MPa, the COD removal rates at HRTs of 16 h and 24 h were relatively high, reaching approximately 92%. However, at an HRT of 10 h, the removal rate was relatively low and fluctuated significantly. This can be attributed to the instability of the biofilm in the initial reaction stage, consistent with the findings of Wang (2012), who reported similar issues with biofilm stability affecting pollutant removal in their studies. During this period, the biofilm was still developing, and the microbial communities had not yet established a stable metabolic equilibrium. As a result, the degradation of organic matter, which contributes to COD, was less efficient. As the reaction progressed, the COD removal rate increased when the HRT was longer, indicating that the biofilm was gradually stabilizing, and the microorganisms were adapting to the environmental conditions, thereby enhancing their ability to degrade organic pollutants.

At an oxygen pressure of 0.122 MPa, the COD removal rate further increased to around 94%, with higher values at HRTs of 16 h and 24 h. This enhanced removal efficiency might be due to an optimized balance between the activities of aerobic and anaerobic bacteria. Wei *et al.* (2012) found that a suitable oxygen supply can promote the coordinated operation of aerobic and anaerobic processes in biofilm systems. Under this oxygen pressure, the aerobic bacteria in the inner layers of the biofilm could efficiently oxidize

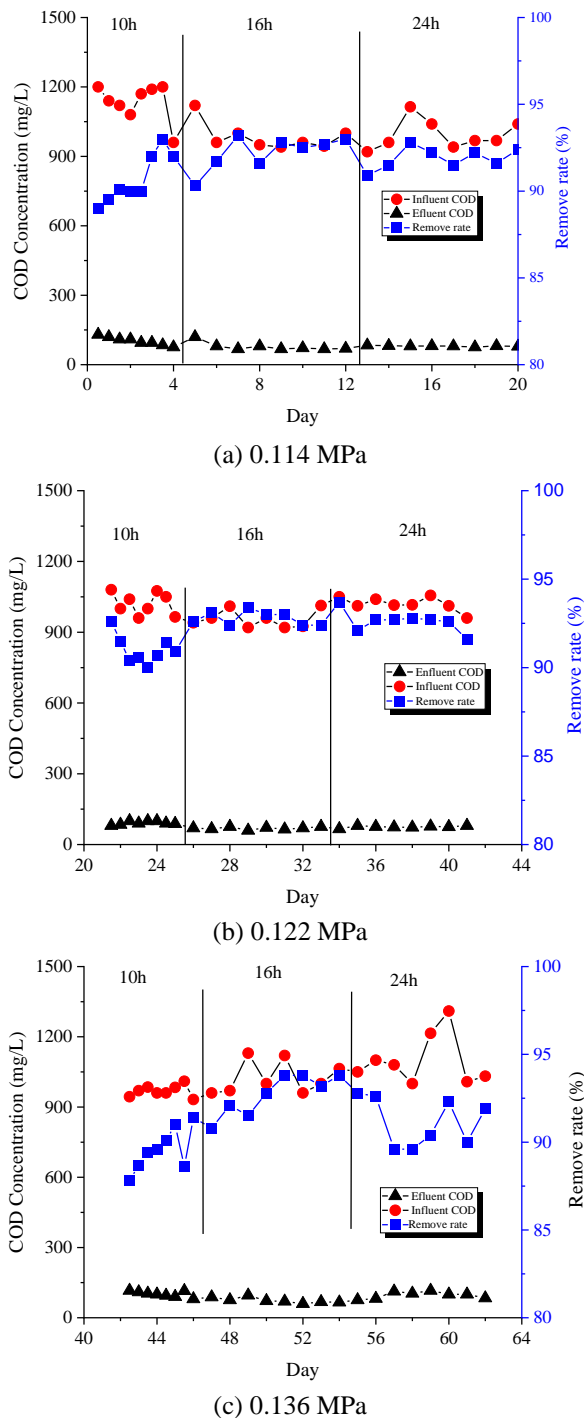


Fig. 5 Effects of different oxygen pressures on COD removal

organic matter using the supplied oxygen. Simultaneously, the anaerobic bacteria in the outer layers of the biofilm could carry out denitrification and other anaerobic metabolic processes. The harmonious coexistence and cooperation of these two types of bacteria likely led to a more comprehensive degradation of organic substances, resulting in a higher COD removal rate.

When the oxygen pressure was elevated to 0.136 MPa, the COD removal rate slightly decreased to an average of about 92%. The increase in oxygen pressure might have

disrupted the delicate ecological balance within the biofilm. High oxygen concentrations could have inhibited the activity of anaerobic bacteria in the inner layers of the biofilm, as Machat *et al.* (2019) demonstrated in their research on the impact of oxygen levels on anaerobic bacteria in biological reactors. Anaerobic bacteria play a crucial role in the degradation of certain complex organic compounds through anaerobic digestion and fermentation processes. With their activity compromised, the overall degradation of organic matter was affected, leading to a reduction in the COD removal rate.

In general, the most favorable COD removal effect was achieved at an HRT of 16 h and an oxygen pressure of 0.122 MPa. At this combination of conditions, the balance between nitrification and denitrification was likely optimized. When the oxygen pressure was too low, the activity of anaerobic bacteria was relatively high, resulting in a greater amount of denitrification. Conversely, when the oxygen pressure was too high, aerobic bacteria became more dominant, and nitrification prevailed. The highest removal efficiency was attained when the difference between nitrification and denitrification was minimal, which occurred around an oxygen pressure of 0.122 MPa. Additionally, when the HRT was extended, the removal rate might have decreased because the extended retention time could lead to a depletion of organic matter in the reactor, as suggested by Fu *et al.* in their study on the impact of HRT on nutrient removal in wastewater treatment systems (Fu *et al.* 2009). As a result, there was insufficient substrate to support the metabolic activities of the microorganisms, thereby reducing the COD removal rate.

### 3.4 Removal rate of TN

The Total Nitrogen (TN) before and after degradation is shown in Fig. 6. At an oxygen pressure of 0.114 MPa, it can be clearly seen that the TN removal rate is the lowest at an HRT of 10 h, around 80%, and at HRTs of 16 h and 24 h, the TN removal rates are approximately 85% and 84%, respectively. From the figure, it can be observed that the TN removal rate fluctuates greatly and is relatively low in the first few days of the reaction, which may be due to the instability of the biofilm. This is because, in the early stages of starting up a membrane aerated biological reactor, the biofilm has not yet fully formed, resulting in low stability and removal rates.

Although we did not measure  $\text{NO}_3^-$ -N, the low and fluctuating TN removal rates at 0.114 MPa, especially at an HRT of 10 h, suggest that the biofilm instability likely affected both nitrification and denitrification processes. The limited oxygen supply might have hindered the activity of nitrifying bacteria, leading to incomplete conversion of ammonium to nitrate. Additionally, the unstable biofilm structure could have disrupted the anoxic environment necessary for efficient denitrification.

At an oxygen pressure of 0.122 MPa, the TN removal rate is highest at an HRT of 16 h, reaching 88%, and at an HRT of 24 h, the removal rate is around 86%. Compared to an HRT of 24 h, the degradation rate does not change significantly, and the removal rate is also relatively stable, indicating that the biofilm has stably formed and the

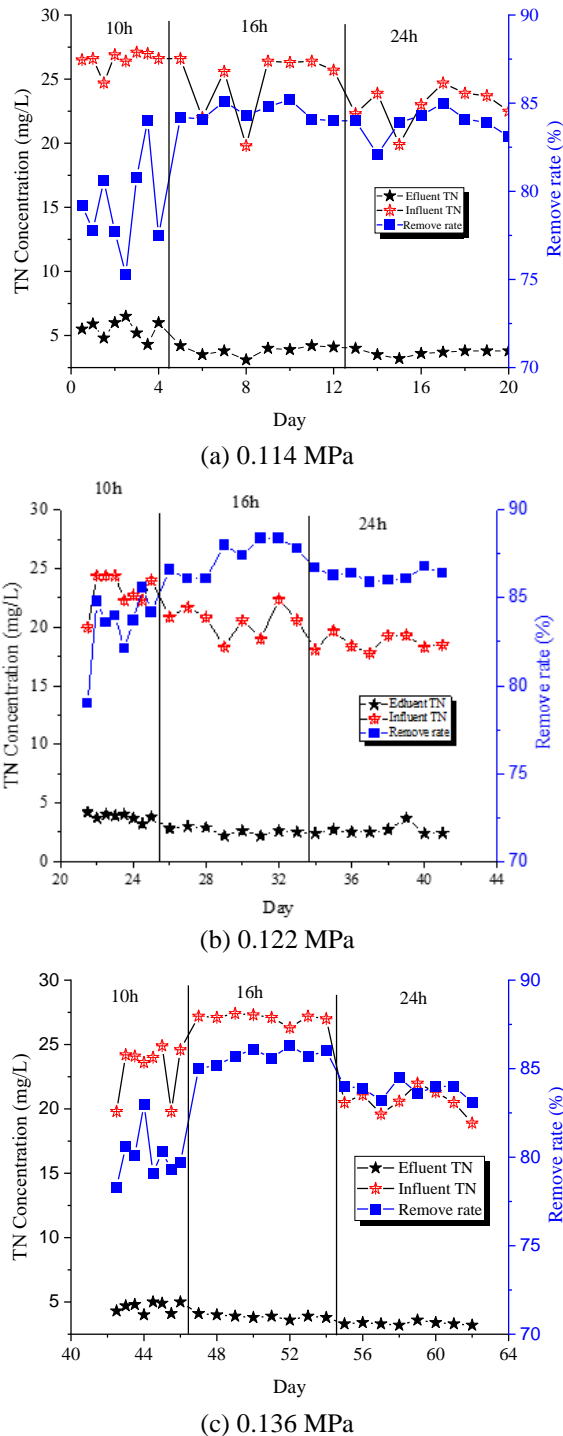


Fig. 6 Effects of different oxygen pressures on TN removal

biological activity is high.

It is likely that at 0.122 MPa, a better balance between nitrification and denitrification was achieved. The increased oxygen supply could have enhanced the activity of nitrifying bacteria, facilitating the conversion of ammonium to nitrate. Meanwhile, the stable biofilm structure and sufficient carbon source likely supported the denitrifying bacteria in reducing nitrate to nitrogen gas. However, without measuring  $\text{NO}_3^-$ -N, this remains an inference based on the observed TN removal rates.

At an oxygen pressure of 0.136 MPa, the TN removal rate slightly decreases, with TN removal rates at HRTs of 16 h and 24 h being around 84% and 86%, respectively. The main reason for the lower removal rate at this time is the high oxygen pressure, which causes the biofilm to become unstable due to pressure impact.

The high oxygen pressure might have penetrated deep into the biofilm, reducing the size of the anoxic zone where denitrification occurs. This could have inhibited the activity of denitrifying bacteria, leading to a decrease in the TN removal rate. Although the absence of  $\text{NO}_3^-$ -N data prevents a definitive conclusion, this hypothesis is consistent with the observed trend in TN removal.

From the figure, it can be seen that at an oxygen pressure of 0.122 MPa and an HRT of 16 h, the TN removal rate is the highest, and the removal rate does not change significantly at HRTs of 16 h and 24 h. Under the three different oxygen pressures, the TN removal rate at an HRT of 10 h fluctuates greatly. The main reason for the low and unstable removal rate at 0.114 MPa is that the MABR has just started, and the biofilm has not fully formed, making everything unstable. At an oxygen pressure of 0.122 MPa, it can be seen from the figure that there is a large difference between the first and second data measurements, mainly because the biofilm has not fully adapted to the change in oxygen pressure. At an oxygen pressure of 0.136 MPa, the main reason for the lower removal rate is that high oxygen pressure leads to biofilm instability (Layer *et al.* 2020).

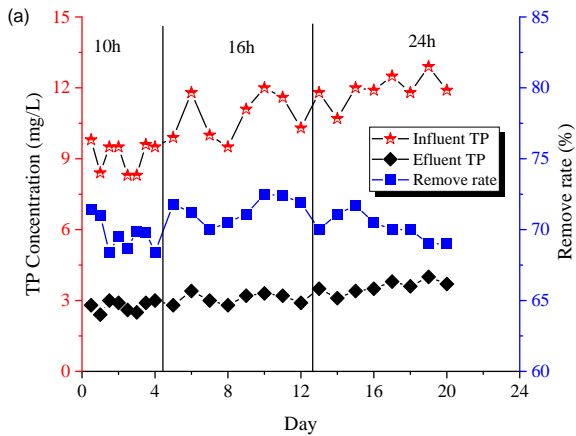
At an oxygen pressure of 0.136 MPa, the TN removal rate slightly decreased. The TN removal rates at HRTs of 16 h and 24 h were around 84% and 86%, respectively. The high oxygen pressure disrupts the biofilm structure, causing it to become unstable. Excessive oxygen penetrates deep into the biofilm, reducing the size of the anoxic zone where denitrification occurs. As a result, the denitrifying bacteria are less able to function effectively, leading to a decrease in the TN removal rate.

In summary, Fig. 6 clearly shows that the highest TN removal rate was achieved at an oxygen pressure of 0.122 MPa and an HRT of 16 h. Under the three different oxygen pressures, the TN removal rate at an HRT of 10 h fluctuated greatly due to the combined effects of limited contact time and biofilm instability. The data emphasize the importance of optimizing both oxygen pressure and HRT to achieve efficient TN removal in the membrane aerated biofilm reactor, as the stability and activity of the biofilm are highly influenced by these parameters (Layer *et al.* 2020).

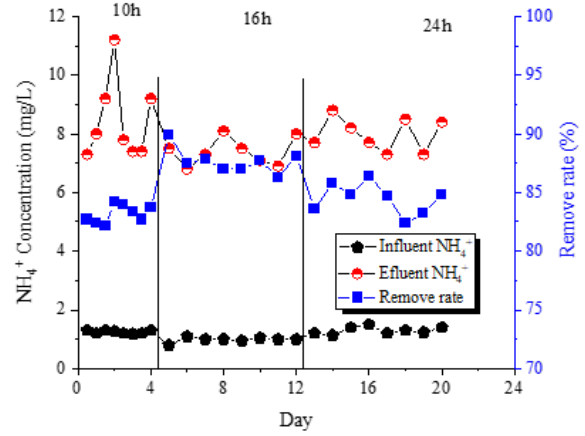
As described in the experimental design section, the reactors were considered to reach a steady state based on the stability of the pollutant removal rates. The differences in operation durations under different HRTs were crucial for revealing the complex behavior of the system. From the data presented in Figs. 5 and 6 it can be seen that COD and TN concentrations are not stable, which further validates the significance of our experimental approach.

### 3.5 Removal Rate of TP

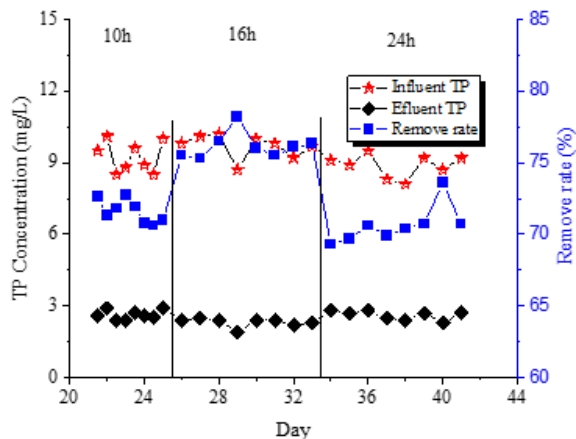
When it comes to TP removal in the MABR system (Fig. 7), indeed, explaining the mechanisms solely based on



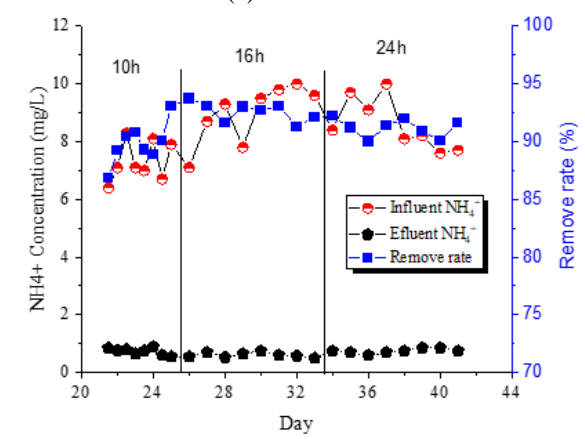
(a) 0.114 MPa



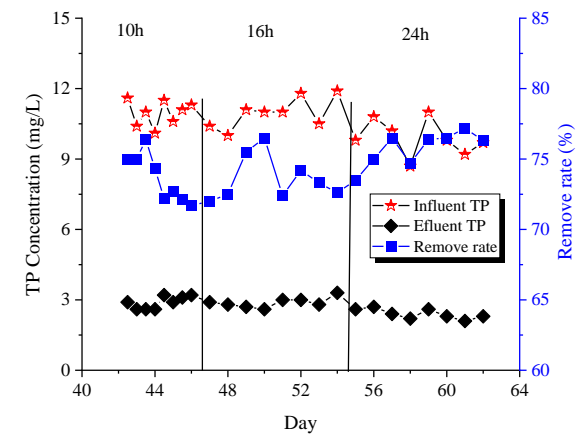
(a) 0.114 MPa



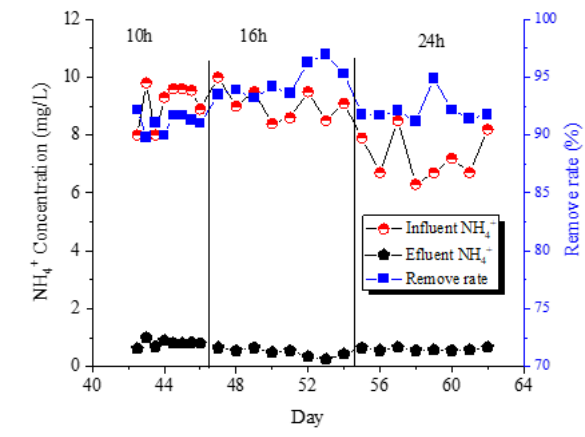
(b) 0.122 MPa



(b) 0.122 MPa



(c) 0.136 MPa



(c) 0.136 MPa

Fig. 7 Effects of different oxygen pressures on TP removal

Fig. 8 Effects of different oxygen pressures on  $\text{NH}_4^+\text{-N}$  removal

operating factors such as oxygen pressure and HRT presents challenges.

Oxygen pressure's impact on TP removal is complex. At an oxygen pressure of 0.114 MPa, HRT had no significant effect on TP removal, with the highest removal rate around 72% at an HRT of 16 h and remaining similar at 24 h. The insufficiency of nutrients likely contributed to the stable removal rate. However, at an HRT of 10 h, the TP removal rate was lowest, which could be due to biofilm instability. When the oxygen pressure increased to 0.122

MPa, the TP removal efficiency peaked at an HRT of 16 h, reaching around 78%. This indicates that under this oxygen pressure, the biofilm was more stable and microbial activity was higher. But the reasons behind this are not straightforwardly linked to oxygen pressure itself. It might be that the optimal oxygen pressure promotes the growth and activity of phosphate-accumulating organisms (PAOs), which play a crucial role in biological phosphorus uptake. Under aerobic conditions, PAOs take up and store phosphate

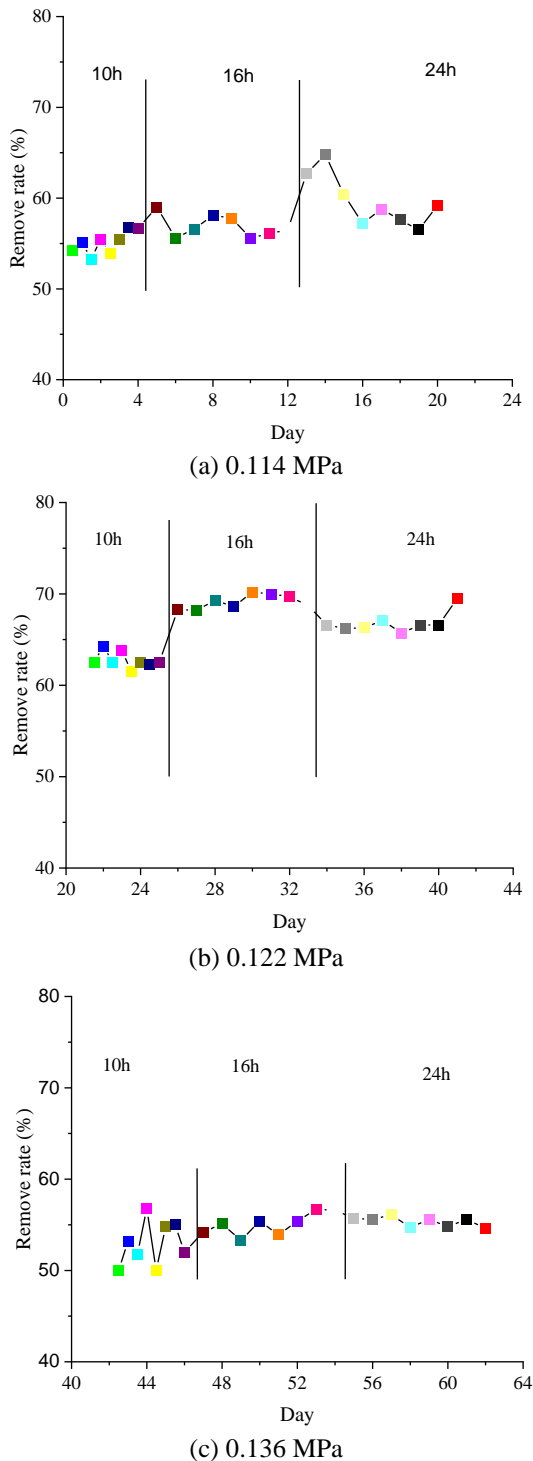


Fig. 9 Effects of different oxygen pressures on TC degradation

intracellularly, and use this stored phosphate under anaerobic conditions and take up more when back in aerobic states (Filipe *et al.* 2001). However, it's hard to directly attribute the changes in TP removal to oxygen pressure without further in-depth research on the specific physiological responses of PAOs to different oxygen levels.

HRT also affects TP removal, but the relationship is not easily explained. Although the highest TP removal rate was

achieved at an HRT of 16 h under certain oxygen pressures, the reasons are not simply due to the length of contact time. Longer HRTs might not necessarily lead to higher TP removal rates. For example, at an oxygen pressure of 0.114 MPa, the TP removal rate remained relatively stable between HRTs of 16 h and 24 h. This could be because other factors, such as the availability of nutrients and the balance of microbial communities, play significant roles. Additionally, the biofilm's ability to adsorb phosphate ions due to its large surface area and functional groups, as well as the sequestration of phosphate by extracellular polymeric substances (EPS) in the biofilm (Zeng *et al.* 2019), are also involved in the TP removal process. These mechanisms are influenced by multiple factors simultaneously, making it difficult to isolate the impact of HRT.

In conclusion, while oxygen pressure and HRT do impact TP removal, the underlying mechanisms are intertwined with various biological, chemical, and physical processes within the MABR system.

In the MABR system, phosphorus (P) removal occurs through multiple mechanisms. Chemical precipitation plays a part when metal ions like calcium, iron, or aluminum in wastewater react with phosphate ions to form insoluble compounds (Pratt *et al.* 2012); Biological uptake by phosphate-accumulating organisms (PAOs) is crucial, under aerobic conditions, PAOs take up and store phosphate intracellularly, they use this stored phosphate under anaerobic conditions and take up more when back in aerobic states (Filipe *et al.* 2001); The biofilm also contributes, it adsorbs phosphate ions due to its large surface area and functional groups, additionally extracellular polymeric substances (EPS) in the biofilm can complex with phosphate, sequestering it (Zeng *et al.* 2019). These combined mechanisms work together to remove P from the wastewater in the MABR system.

### 3.6 Removal Rate of $\text{NH}_4^+\text{-N}$

The removal of  $\text{NH}_4^+\text{-N}$  before and after treatment is shown in Fig. 8. At an oxygen pressure of 0.114 MPa, the maximum removal rate was around 90%. At an HRT of 10 h, the  $\text{NH}_4^+\text{-N}$  removal rate was the lowest, at approximately 82%, which may be due to the short HRT and could also be influenced by the instability of the biofilm in the early stages of the reaction. At an HRT of 16 h, the  $\text{NH}_4^+\text{-N}$  removal rate was the highest, at about 88%, indicating that the biofilm was relatively stable at this time and the reaction was faster. At an HRT of 24 h, the  $\text{NH}_4^+\text{-N}$  removal rate slightly decreased, possibly because the longer HRT led to a shortage of organic matter required by bacteria in the later stages of the reaction, resulting in a lower removal rate.

At an oxygen pressure of 0.122 MPa, the  $\text{NH}_4^+\text{-N}$  removal rates under the three HRT conditions did not change significantly and tended to be stable. The  $\text{NH}_4^+\text{-N}$  removal rates at HRTs of 16 h and 24 h reached around 92%, and at an HRT of 10 h, the  $\text{NH}_4^+\text{-N}$  removal rate was around 90%. At this time, the oxygen pressure conditions were optimal, the biofilm was stable, and the nitrification and denitrification reactions were not significantly different.

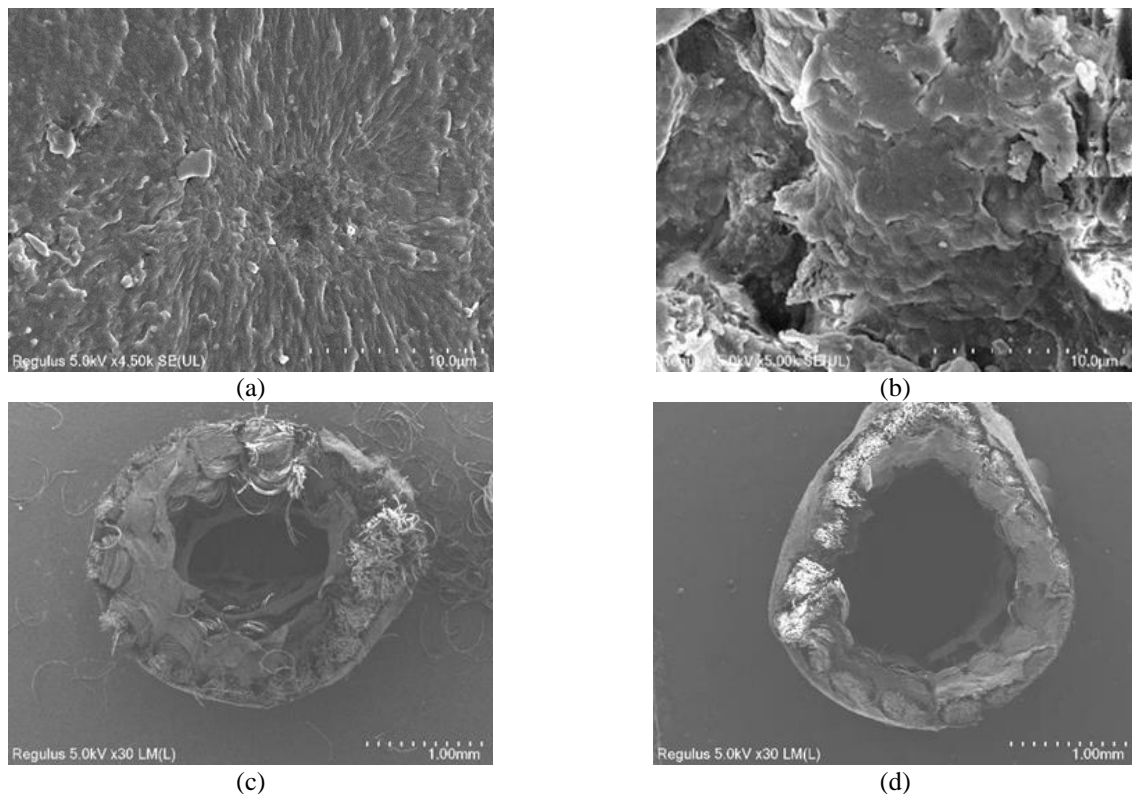


Fig. 10 Surfaces of hollow fiber membrane before and after using (a and b), Cross-section of hollow fiber membrane before and after using (c and d)

### 3.7 Removal rate of tetracycline

The degradation of tetracycline (TC) before and after degradation is shown in Fig. 9. From the three sets of figures, it can be seen that HRT has little effect on the degradation of TC. Similarly, the degradation rate of TC is not high at the beginning of the reaction, and the degradation rate is unstable later, which may both be due to the stability of the biofilm. When the oxygen pressure is 0.122 MPa, the degradation rate of TC increases significantly, indicating that the oxygen pressure has a greater impact on the degradation rate of TC, and the optimal oxygen pressure is around 0.122 MPa, with the highest degradation rate of about 70%.

Compared with the degradation of other substances, the degradation rate of TC is relatively low, but the concentration of TC in the water body is originally low (Yi *et al.* 2020). When the oxygen pressure is 0.114 MPa, the overall degradation rate of TC is around 56%, and the degradation rate of TC is unstable when HRT is 24 h, which may be due to the large error in the experimental data. When the oxygen pressure is 0.136 MPa, the average degradation rate of TC is around 55%, and the degradation rate changes greatly when HRT is 10 h, which may be because the pressure just increased to 0.136 MPa, which has a certain impact on the stability of the biofilm, and then the stability of the biofilm slowly improved (Nasseri *et al.* 2017), when HRT is 16 h and 24 h, the degradation rate of TC is around 56%, from which it can also be seen that HRT has little effect on the degradation of TC.

### 3.8 MABR Evaluation

Through the analysis of the above points, it can be concluded that HRT has little impact on the degradation of wastewater, while the pressure of oxygen has a greater influence on the degradation. Therefore, it is necessary to control the oxygen pressure near the optimal conditions during actual degradation treatment. Although there is not much difference in the degradation effect between HRTs of 16 h and 24 h, the maximum benefit is achieved when the HRT is 16 h (Bodkhe, 2009). Among all substances degraded, the remove rate of COD is relatively higher. The organic loading rate of the MABR, as measured and calculated, is 1.062 kg/m<sup>3</sup>.d. Although the degradation rate of TC is only about 70% at its highest, it is still relatively high compared to other biological degradation methods.

The MABR exhibited relatively lower efficiency in phosphorus removal compared to other pollutants, consistent with reports in literature where operational factors (e.g., oxygen diffusion depth, HRT) may limit phosphorus accumulation mechanisms. In Fig. 10, the SEM images before the wastewater treatment clearly show a relatively smooth surface with a certain number of pores on the hollow fiber membrane, as described in the text. After the wastewater treatment, the images display the formation of a biofilm, which can be observed as a layer covering the membrane surface. Additionally, the cross-sectional views in Fig. 10 (c) and 1(d) indeed reveal that the side of the hollow fiber membrane becomes more compact, and the number of visible pores decreases, aligning precisely with

our textual description. Overall, the MABR has a significant degradation effect on wastewater, with high degradation rates for various substances, making it a very effective degradation method.

#### 4. Conclusions

This study demonstrates that optimized MABR operation (0.122 MPa aeration, 16-h HRT) effectively treats tetracycline and nutrient-laden wastewater through stratified biofilm processes. Key achievements include:

- 70% tetracycline biodegradation via microbial synergy
- High simultaneous nutrient removal (90%  $\text{NH}_4^+\text{-N}$ , 88% TN, 75% TP)

- 93% COD reduction confirming organic mineralization

The MABR's membrane-aerated design enables energy-efficient oxygen delivery while supporting concurrent nitrification, denitrification, and antibiotic degradation. This positions MABR as a sustainable solution for complex wastewater streams. Future work will focus on system scale-up and phosphorus removal enhancement.

#### Acknowledgements

The research described in this paper was financially supported by a Technology Development Project from Anhui HuaShang Cable Technology Co., Ltd (No. 901/ 852405).

#### References

- Abu Hasan, H., Muhammad, M.H. and Ismail, N.I. (2020), "A review of biological drinking water treatment technologies for contaminants removal from polluted water resources", *J. Water Proc. Eng.*, **33**. <https://doi.org/10.1016/j.jwpe.2019.101035>.
- Ahmed, S.M., Zhou, B.X., Wang, Y., Yang, H., Zheng, Y.P. and Xia, S.B. (2020), "Preparation, Characterization of activated carbon fiber (ACF) from loofah and its application in composite vertical flow constructed wetlands for Tetracycline removal from water", *Membr. Water Treat.*, **11**(4), 313-321. <https://doi.org/10.12989/mwt.2020.11.4.313>.
- Alonso, V.A. and Lackner, S. (2019), "Membrane Aerated Biofilm Reactors - How longitudinal gradients influence nitrogen removal - A conceptual study", *Water Res.*, **166**. <https://doi.org/10.1016/j.watres.2019.115060>.
- Bodkhe, S.Y. (2009), "A modified anaerobic baffled reactor for municipal wastewater treatment", *J. Environ. Manage*, **90**(8), 2488-2493. <https://doi.org/10.1016/j.jenvman.2009.01.007>.
- Celik, A., Casey, E. and Hasar, H. (2018), "Degradation of oxytetracycline under autotrophic nitrifying conditions in a membrane aerated biofilm reactor and community fingerprinting", *J. Hazard. Mater.*, **356**, 26-33. <https://doi.org/10.1016/j.jhazmat.2018.05.040>.
- Filipe, C.D.M., Daigger, G.T. and Grady, C.P.L. (2001), "pH as a key factor in the competition between glycogen-accumulating organisms and phosphorus-accumulating organisms", *Water Environ. Res.*, **73**(2), 223-232. <https://doi.org/10.2175/106143001x139209>.
- Fu, Z., Yang, F., Zhou, F. and Xue, Y. (2009), "Control of COD/N ratio for nutrient removal in a modified membrane bioreactor (MBR) treating high strength wastewater", *Bioresour Technol.*, **100**(1), 136-141. <https://doi.org/10.1016/j.biortech.2008.06.006>.
- Ghasemi, M., Chang, S. and Sivaloganathan, S. (2023), "Modeling and simulation study of simultaneous nitrification-denitrification in membrane aerated bioreactor", *J. Membr. Sci.*, **668**. <https://doi.org/10.1016/j.memsci.2022.121210>.
- Layer, M., Villodres, M.G., Hernandez, A., Reynaert, E., Morgenroth, E. and Derlon, N. (2020), "Limited simultaneous nitrification-denitrification (SND) in aerobic granular sludge systems treating municipal wastewater: Mechanisms and practical implications", *Water Res.*, **X7**, 100048. <https://doi.org/10.1016/j.wroa.2020.100048>.
- Machat, H., Boudokhane, C., Roche, N. and Dhaouadi, H. (2019), "Effects of C/N Ratio and DO concentration on carbon and nitrogen removals in a hybrid biological reactor", *Biochem. Eng. J.*, **151**. <https://doi.org/10.1016/j.bej.2019.107313>.
- Mei, X., Ding, Y., Li, P., Xu, L., Wang, Y., Guo, Z., Shen, W., Yang, Y., Wang, Y., Xiao, Y., Yang, X., Liu, Y., Shen, Y., Wu, Y., Jiang, C. and Xue, C. (2020), "A novel system for zero-discharge treatment of high-salinity acetonitrile-containing wastewater: Combination of pervaporation with a membrane-aerated bioreactor", *Chem. Eng. J.*, **384**. <https://doi.org/10.1016/j.cej.2019.123338>.
- Nasseri, S., Mahvi, A.H., Seyedsalehi, M., Yaghmaeian, K., Nabizadeh, R., Alimohammadi, M. and Safari, G.H. (2017), "Degradation kinetics of tetracycline in aqueous solutions using peroxydisulfate activated by ultrasound irradiation: Effect of radical scavenger and water matrix", *J. Molecular Liq.*, **241**, 704-714. <https://doi.org/10.1016/j.molliq.2017.05.137>.
- Pratt, C., Parsons, S.A., Soares, A. and Martin, B.D. (2012), "Biologically and chemically mediated adsorption and precipitation of phosphorus from wastewater", *Curr. Op. Biotech.*, **23**(6), 890-896. <https://doi.org/10.1016/j.copbio.2012.07.003>.
- Tian, H.L., Zhao, J.Y., Zhang, H.Y., Chi, C.Q., Li, B.A. and Wu, X.L. (2015), "Bacterial community shift along with the changes in operational conditions in a membrane-aerated biofilm reactor", *Appl. Microbiol. Biotechnol.*, **99**(7), 3279-3290. <https://doi.org/10.1007/s00253-014-6204-7>.
- Wang, Z., Xu, X., Gong, Z. and Yang, F. (2012), "Removal of COD, phenols and ammonium from Lurgi coal gasification wastewater using A2O-MBR system", *J. Hazard. Mater.*, **235-236**, 78-84. <https://doi.org/10.1016/j.jhazmat.2012.07.012>.
- Wei, X., Li, B., Zhao, S., Qiang, C., Zhang, H. and Wang, S. (2012), "COD and nitrogen removal in facilitated transfer membrane-aerated biofilm reactor (FT-MABR)", *J. Membr. Sci.*, **389**, 257-264. <https://doi.org/10.1016/j.memsci.2011.10.038>.
- Yi, X., Zhu, J., Yan, Y., Cheng, H. and Xu, W. (2020), "Removal of Tetracycline Hydrochloride (TCH) in Simulated Wastewater by Zero-Valent Iron with Ultrasonic Irradiation (US-ZIV)", *Polish J. Environ. Stud.*, **30**(1), 903-916. <https://doi.org/10.15244/pjoes/123825>.
- Yu, H.Y., Xie, Y., Hu, M.X., Wang, J.L., Wang, S.Y. and Xu, Z.K. (2005), "Surface modification of polypropylene microporous membrane to improve its antifouling property in MBR: CO<sub>2</sub> plasma treatment", *J. Membr. Sci.*, **254**(1-2), 219-227. <https://doi.org/10.1016/j.memsci.2005.01.010>.
- Zeng, F., Jin, W. and Zhao, Q. (2019), "Temperature effect on extracellular polymeric substances (EPS) and phosphorus accumulating organisms (PAOs) for phosphorus release of anaerobic sludge", *RSC Adv.*, **9**(4), 2162-2171. <https://doi.org/10.1039/c8ra10048a>.